

## Catalyst-free synthesis of ZnO nanowall networks on Si<sub>3</sub>N<sub>4</sub>/Si substrates by metalorganic chemical vapor deposition

Sang-Woo Kim<sup>a)</sup>

*School of Advanced Materials and System Engineering, Kumoh National Institute of Technology, Gumi, Gyeongbuk 730-701, Korea*

Shizuo Fujita

*International Innovation Center, Kyoto University, Katsura Int'tech Center, Kyodai-Katsura, Nishikyo-ku, Kyoto 615-8510, Japan*

Min-Su Yi

*Department of Materials Science and Engineering, Sangju National University, Sangju, Gyeongbuk 742-711, Korea*

Dae Ho Yoon

*Department of Advanced Materials Engineering, Sungkyunkwan University, Suwon, Kyunggi 440-746, Korea*

(Received 31 January 2006; accepted 10 May 2006; published online 23 June 2006)

ZnO nanowall networks were synthesized on Si<sub>3</sub>N<sub>4</sub>/Si (100) substrates at low growth temperature of 350 °C by metalorganic chemical vapor deposition (MOCVD) without any help of metal catalysts. Depending on MOCVD-growth conditions, a large number of nanowalls with extremely small wall thicknesses below 10 nm are formed into nanowalls with a thickness of about 20 nm, resulting in the formation of two-dimensional nanowall networks. The ZnO nanowall networks were found to have a preferred *c*-axis orientation with a hexagonal structure in synchrotron x-ray scattering experiments. Room-temperature hydrogen incorporation into ZnO nanowall networks has been observed in photoluminescence measurements. © 2006 American Institute of Physics.

[DOI: 10.1063/1.2216107]

ZnO with a wide band of 3.37 eV and large excitonic binding energy of 60 meV is of great interest for photonic applications.<sup>1,2</sup> Recent researches have shown that ZnO exhibits room-temperature (RT) stimulated emission.<sup>3,4</sup> In addition, ZnO is very promising in possible device applications such as hydrogen-storage application,<sup>5</sup> solar cells,<sup>6</sup> chemical sensors,<sup>7,8</sup> and surface acoustic wave devices.<sup>9</sup> ZnO nanostructures such as quantum well,<sup>10</sup> quantum dots,<sup>11</sup> nanowires,<sup>12</sup> nanobelts,<sup>13</sup> nanonails,<sup>14</sup> and nanotubes<sup>15</sup> have been attracting great attention because it is expected that the device performance can be improved by nanostructuring. Recently, several groups have reported on the fabrication of ZnO nanowalls using a vapor-liquid-solid (VLS) process<sup>16,17</sup> with a metal catalyst at high growth temperature of over 900 °C. However, high temperature processes seriously limit device applications and increase thermal strain in the grown nanostructures. Moreover, a broad deep-level emission band is usually observed in ZnO nanostructures grown by a VLS process, indicating that they contain a great number of point defects.<sup>17,18</sup>

ZnO nanowalls grown by metalorganic chemical vapor deposition (MOCVD) have been recently reported without the aid of a catalyst at relatively low growth temperatures (around 500 °C).<sup>19,20</sup> They suggested that ZnO nanowalls can be used in energy-storage devices, chemical and biological sensors, and dye-sensitized solar cells because the total surface area in nanowalls is much larger than that in thin films. However, the density of the ZnO nanowalls in their work is not sufficient to realize above-mentioned devices with high efficiency. Wan *et al.*<sup>5</sup> reported on RT hydrogen-storage characteristics of ZnO nanowires, indicating that re-

alization of high-density ZnO nanowalls is very promising for hydrogen storage because an active surface area of nanowall structures is much larger than that of nanowire structures.

The MOCVD growth for ZnO nanowall networks was carried out on Si<sub>3</sub>N<sub>4</sub> (50 nm)/Si (100) substrates at a pressure of 200 Torr for 30 min. The Si<sub>3</sub>N<sub>4</sub> layer on Si was deposited by plasma-enhanced chemical vapor deposition.<sup>21</sup> Typical flow rates of source materials for the ZnO growth, diethylzinc (DEZn) and N<sub>2</sub>O, were 3–5 and 1250 μmol/min, respectively.<sup>22</sup> The MOCVD-growth temperature of 350 °C was introduced.

Figure 1 shows field-emission scanning electron microscope (FE-SEM) images of ZnO nanowall networks grown on Si<sub>3</sub>N<sub>4</sub> (50 nm)/Si (100) substrates at 350 °C in the MOCVD chamber as a function of DEZn flow rates from 3 to 5 μmol/min. These images show that two-dimensional ZnO nanowall networks were grown vertically on the substrates. It should be pointed out that the average thickness of nanowalls grown with the DEZn flow rate of 5 μmol/min is much smaller than that in previous reports.<sup>16,17,19,20</sup> As shown in Figs. 1(c) and 1(f), a large number of nanowalls with extremely small wall thicknesses (below 10 nm) formed networks into relatively large nanowalls (average nanowall thickness of about 20 nm). The size distribution of the extremely small nanowalls formed into relatively large nanowalls is remarkably uniform over the whole substrate surface area. The DEZn flow rate was found to cause rather drastic changes to the morphology of the nanowall networks, which means that the nanowall density and size are strong functions of the DEZn flow rate, as shown in Fig. 1. The density of the nanowalls increased, and the size of these decreased dramatically by increasing the DEZn flow rate. As shown in Figs.

<sup>a)</sup>Electronic mail: kimsw@kumoh.ac.kr

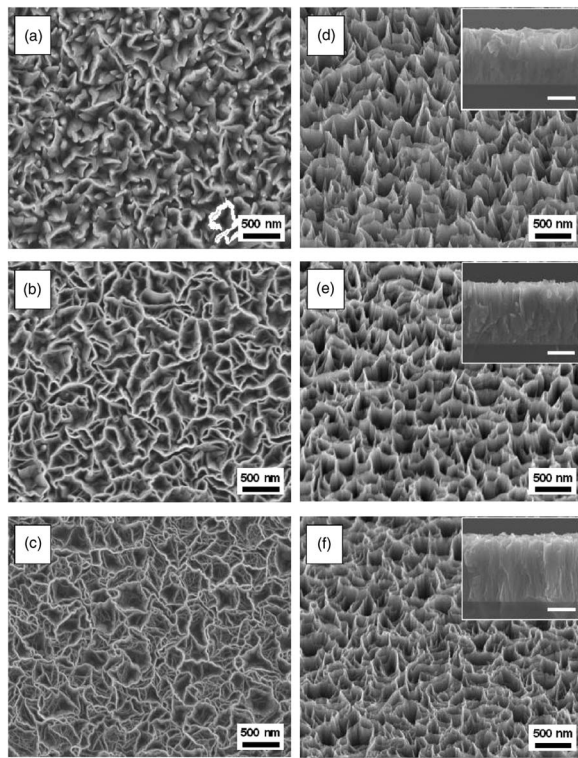


FIG. 1. FE-SEM images of MOCVD-grown ZnO nanowall networks on  $\text{Si}_3\text{N}_4/\text{Si}$  (100) substrates at  $350^\circ\text{C}$  under different DEZn flow rates. [(a), (b), and (c)] Plan-view FE-SEM images of the ZnO nanowall networks with DEZn flow rates of 3, 4, and  $5\ \mu\text{mol}/\text{min}$ , respectively. [(d), (e), and (f)] Tilting-view FE-SEM images of (a), (b), and (c) samples, respectively. Insets show cross-sectional FE-SEM images of the ZnO nanowall networks on  $\text{Si}_3\text{N}_4/\text{Si}$  (100) substrates. A scale bar in the insets indicates 500 nm.

1(a) and 1(d), it is difficult to observe the extremely small nanowalls in the sample grown with the DEZn flow rate of  $3\ \mu\text{mol}/\text{min}$ . This fact indicates that zinc atoms play an important role in the formation of nanowall networks with high density. The average heights of ZnO nanowall networks are 950 nm,  $1.1\ \mu\text{m}$ , and  $1.2\ \mu\text{m}$ , respectively, as shown in the insets of Figs. 1(d)–1(f).

Figures 2(a) and 2(b) show the diffraction profiles of the ZnO nanowall samples grown with the DEZn flow rate of 3 and  $5\ \mu\text{mol}/\text{min}$ , respectively, along the substrate normal direction in reciprocal space measured by typical  $\theta$ - $2\theta$  scans [ $Q=4\pi\sin(2\theta/2)/\lambda$ ]. The diffraction peak of the ZnO nanowall networks grown with the DEZn flow rate of  $5\ \mu\text{mol}/\text{min}$  occurs only at  $2.41\ \text{\AA}^{-1}$  which is related with the ZnO (0002) Bragg reflection [Fig. 2(b)], while the ZnO nanowall networks grown with the DEZn flow rate of  $3\ \mu\text{mol}/\text{min}$  not only have the ZnO (0002) Bragg reflection but also the ZnO (10 $\bar{1}$ 0) and ZnO (10 $\bar{1}$ 1) Bragg reflections [Fig. 2(a)]. The diffraction profile is measured in the  $\langle 2.1\ \text{\AA}^{-1}0l \rangle$  direction in reciprocal space, keeping in-plane momentum transfer at the reciprocal of the in-plane lattice spacing to study the stacking order of the grown ZnO nanowall networks.<sup>23</sup> The cubic (11 $\bar{1}$ ) and cubic (002) reflections would occur at  $(2.1, 0, 0.8\ \text{\AA}^{-1})$  and  $(2.1, 0, 1.6\ \text{\AA}^{-1})$ , respectively, while the hexagonal (10 $\bar{1}$ 1) reflection would occur at  $(2.1, 0, 1.2\ \text{\AA}^{-1})$ . Therefore, we could conclude that the crystal structure of both samples is hexagonal, as shown in Figs. 2(c) and 2(d).

Effects of the DEZn flow rate on the crystal quality and surface morphology of ZnO thin films on Si substrates have

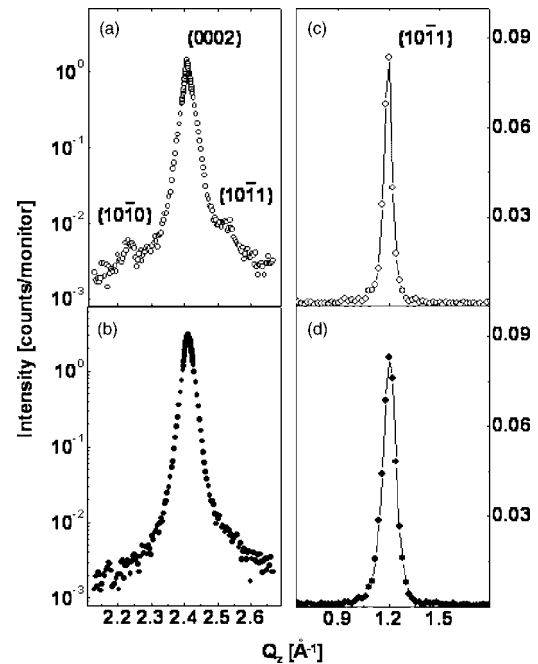


FIG. 2. [(a) and (b)] Powder diffraction profiles along the substrate normal direction in reciprocal space measured on the ZnO nanowall networks grown with the DEZn flow rate of 3 and  $5\ \mu\text{mol}/\text{min}$ , respectively. [(c) and (d)] Scattering profiles along the  $\langle 2.1\ \text{\AA}^{-1}0l \rangle$  direction from the samples of Figs. 2(a) and 2(b), respectively. They are sensitive to the stacking sequence of the atomic layers of ZnO nanowall networks.

been investigated in a previous research (which will be published elsewhere). When the DEZn flow increases, the  $c$ -axis oriented crystallinity is improved, but the surface smoothness deteriorates, which indicates that ZnO grows three dimensionally in a high DEZn flow rate. In the growth condition of a high DEZn flow rate, a large number of zinc adatoms incorporate and effectively form ZnO nuclei on  $\text{Si}_3\text{N}_4/\text{Si}$  (100) substrates, resulting in the formation of nanowalls with an extremely small wall thickness and a high density as well as a preferred  $c$ -axis crystal orientation. Therefore, an average height of the nanowall networks increases with the increment of a DEZn flow rate, as shown in the insets of Fig. 1.

We measured the azimuth scan at the nonspecular ZnO (10 $\bar{1}$ 1) Bragg peak position to study structural correlation between substrates and ZnO nanowall networks (not shown). From the experiment, it could be concluded that both samples have no epitaxial relationship between substrates and ZnO nanowall networks, but a preferred  $c$ -axis growth behavior of ZnO on  $\text{Si}_3\text{N}_4/\text{Si}$  substrates due to the amorphous  $\text{Si}_3\text{N}_4$  layer on Si. Although the formation mechanism of catalyst-free MOCVD-grown nanowall networks on  $\text{Si}_3\text{N}_4/\text{Si}$  substrates is not described clearly in the present study, relaxation of the lattice mismatch strain induced by the absence of epitaxial relation between ZnO and the  $\text{Si}_3\text{N}_4$  layer may play a key role in the formation of the ZnO nanowall networks.

The influence of the  $\text{H}_2$  treatment to optical properties of the ZnO nanowall networks was investigated by photoluminescence (PL) measurements using excitation at the 325 nm line of a He–Cd laser as an excitation source. Figure 3 shows PL spectra of the as-grown nanowall-network samples [shown in Figs. 1(a) and 1(c)] and  $\text{H}_2$ -treated nanowall-network samples. Hydrogenation [ $\text{H}_2$  flow rate: 1000 SCCM

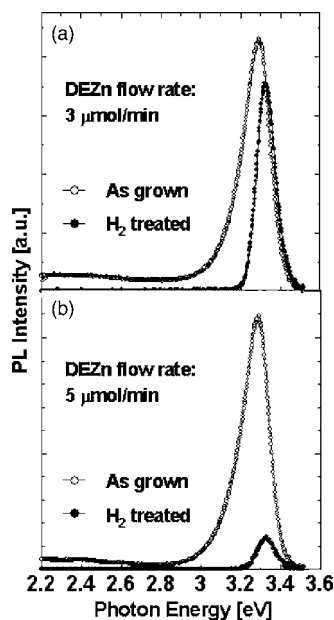


FIG. 3. PL spectra of ZnO nanowall networks measured at RT. (a) DEZn flow rate of  $3 \mu\text{mol}/\text{min}$ : as-grown sample and  $\text{H}_2$ -treated sample. (b) DEZn flow rate of  $5 \mu\text{mol}/\text{min}$ : as-grown sample and  $\text{H}_2$ -treated sample.

(standard cubic centimeter per minute)] was carried out in the MOCVD chamber under a pressure of about 0.1 MPa (760 Torr) for 90 min at RT. Each as-grown ZnO nanowall sample clearly shows ultraviolet near-band-edge emission around 3.29 eV and broad deep-level emission around 2.4 eV, while the near-band-edge emission band strongly quenches and the deep-level emission band disappears in both samples after hydrogenation. The intensity of near-band-edge emission from the hydrogenated nanowall-network sample (grown with the DEZn flow rate of  $5 \mu\text{mol}/\text{min}$ ) with extremely small nanowalls is very weak (about eight times weaker than the intensity of near-band-edge emission from the as-grown sample), as shown in Fig. 3(b), which might be attributed to enlarged surface areas for favorable hydrogen incorporation.

The absorption of hydrogen on a bulk ZnO surface has been investigated based on the applications of ZnO in hydrogen sensing.<sup>24,25</sup> Hence, we believe that the major process behind the interaction between the nanowalls and hydrogen is the chemisorption of the dissociated hydrogen on the ZnO nanowall surface. Of course, we should not exclude the possibility of physisorption of hydrogen into nanosized holes or pores which might be present on the nanowall surface. Hydrogen is suspected of forming a shallow donor state.<sup>26,27</sup> Thus incorporated hydrogen atoms during hydrogenation could introduce a large number of nonradiative recombination centers, resulting in strong quenching of the near-band-edge emission.<sup>5</sup> Furthermore, the near-band-edge of the hydrogenated nanowall samples shifts toward higher energies compared to that of the as-grown samples, which is likely due to the Burstein-Moss effect.<sup>28,29</sup> In addition, disappearance of the deep-level emission band after hydrogenation in accordance with the results in the previous reports might be attributed to hydrogen passivation of point defects such as oxygen vacancies causing deep-level emission.<sup>5,30</sup> However, the intensity of the near-band edge-emission from the hydrogenated sample [shown in Fig. 3(b)] was almost recovered by thermal annealing at  $200^\circ\text{C}$  comparable to that of the near-band-edge emission from the as-grown sample.

In summary, catalyst-free synthesis of ZnO nanowall networks on  $\text{Si}_3\text{N}_4$  (50 nm)/Si (100) substrates at low growth temperature of  $350^\circ\text{C}$  by MOCVD without catalyst driving was reported in this work. In the MOCVD-growth condition with the DEZn flow rate of  $5 \mu\text{mol}/\text{min}$ , a large number of nanowalls with extremely small wall thicknesses below 10 nm formed networks into nanowalls with a thickness of about 20 nm. The nanowall density, size, and crystal orientation are strong functions of the DEZn flow rate. Hydrogen-storage behavior of the ZnO nanowall networks hydrogenated at RT has been investigated by RT PL measurements, indicating that ZnO nanowall networks are promising in the application of hydrogen-storage devices.

This work was partly supported by a research fund from the Kumoh National Institute of Technology, Project No. 2005-104-107.

- <sup>1</sup>K. Hummer, Phys. Status Solidi B **56**, 249 (1973).
- <sup>2</sup>A. Mang, K. Reimann, and St. Ruhenacke, Solid State Commun. **94**, 251 (1995).
- <sup>3</sup>D. M. Bagnall, Y. F. Chen, Z. Zhu, T. Yao, M. Y. Shen, and T. Goto, Appl. Phys. Lett. **73**, 1038 (1998).
- <sup>4</sup>A. Ohtomo, K. Tamura, M. Kawasaki, T. Makino, Y. Segawa, Z. K. Tang, G. K. L. Wong, Y. Matsumoto, and H. Koinuma, Appl. Phys. Lett. **77**, 2204 (2000).
- <sup>5</sup>Q. Wan, C. L. Lin, X. B. Yu, and T. H. Wang, Appl. Phys. Lett. **84**, 124 (2004).
- <sup>6</sup>J. B. Baxter and E. S. Aydil, Appl. Phys. Lett. **86**, 053114 (2005).
- <sup>7</sup>Z. Fan and J. G. Lu, Appl. Phys. Lett. **86**, 123510 (2005).
- <sup>8</sup>Z. Fan, D. Wang, P. Chang, W. Tseng, and J. G. Lu, Appl. Phys. Lett. **85**, 5923 (2004).
- <sup>9</sup>C. R. Gorla, N. W. Emanetoglu, S. Liang, W. E. Mayo, Y. Lu, M. Wraback, and H. Shen, J. Appl. Phys. **85**, 2595 (1999).
- <sup>10</sup>Th. Gruber, C. Kirchner, R. Kling, F. Reuss, and A. Waag, Appl. Phys. Lett. **84**, 5359 (2004).
- <sup>11</sup>S.-W. Kim, Sz. Fujita, and Sg. Fujita, Appl. Phys. Lett. **81**, 5036 (2002).
- <sup>12</sup>M. H. Huang, S. Mao, H. Feick, H. Yan, Y. Wu, H. Kind, E. Weber, R. Russo, and P. Yang, Science **292**, 1897 (2001).
- <sup>13</sup>Z. W. Pan, Z. R. Dai, and Z. L. Wang, Science **291**, 1947 (2001).
- <sup>14</sup>J. Y. Lao, J. Y. Huang, D. Z. Wang, and Z. F. Ren, Nano Lett. **3**, 235 (2003).
- <sup>15</sup>J.-J. Wu, S.-C. Liu, C.-T. Wu, K.-H. Chen, and L.-C. Chen, Appl. Phys. Lett. **81**, 1312 (2002).
- <sup>16</sup>H. T. Ng, J. Li, M. K. Smith, P. Nguyen, A. Cassell, J. Han, and M. Meyyappan, Science **300**, 1249 (2003).
- <sup>17</sup>J. Y. Lao, J. Y. Huang, D. Z. Wang, Z. F. Ren, D. Steeves, B. Kimball, and W. Porter, Appl. Phys. A: Mater. Sci. Process. **A78**, 539 (2004).
- <sup>18</sup>M. H. Huang, Y. Wu, H. Feick, N. Tran, E. Weber, and P. Yang, Adv. Mater. (Weinheim, Ger.) **13**, 113 (2001).
- <sup>19</sup>B. P. Zhang, K. Wakatsuki, N. T. Binh, Y. Segawa, and N. Usami, J. Appl. Phys. **96**, 340 (2004).
- <sup>20</sup>B. P. Zhang, N. T. Binh, K. Wakatsuki, Y. Segawa, Y. Yamada, N. Usami, M. Kawasaki, and H. Koinuma, J. Phys. Chem. B **108**, 10899 (2004).
- <sup>21</sup>C.-C. Lin, S.-Y. Chen, S.-Y. Cheng, and H.-Y. Lee, Appl. Phys. Lett. **84**, 5040 (2004).
- <sup>22</sup>S.-W. Kim, Sz. Fujita, and Sg. Fujita, Appl. Phys. Lett. **86**, 153119 (2005).
- <sup>23</sup>M. S. Yi, H. H. Lee, D. J. Kim, S. J. Park, D. Y. Noh, C. C. Kim, and J. H. Je, Appl. Phys. Lett. **75**, 2187 (1999).
- <sup>24</sup>K. D. Mitzner, J. Sternhagen, and D. W. Galipeau, Sens. Actuators B **93**, 92 (2003).
- <sup>25</sup>A. A. Tomchenko, G. P. Harmer, B. T. Marquis, and J. W. Allen, Sens. Actuators B **93**, 126 (2003).
- <sup>26</sup>C. G. Van de Walle, Phys. Rev. Lett. **85**, 1012 (2000).
- <sup>27</sup>K. Shimomura, K. Nishiyama, and R. Kadono, Phys. Rev. Lett. **89**, 255505 (2002).
- <sup>28</sup>N. Y. Lee, K.-J. Lee, C. Lee, J.-E. Kim, H. Y. Park, D.-H. Kwak, H.-C. Lee, and H. Lim, J. Appl. Phys. **78**, 3367 (1995).
- <sup>29</sup>L.-Y. Chen, W.-H. Chen, J.-J. Wang, F. Hong, and Y.-K. Su, Appl. Phys. Lett. **85**, 5628 (2004).
- <sup>30</sup>I. Ozerov, M. Arab, V. I. Safarov, W. Marine, S. Giorgio, M. Sentis, and L. Nanai, Appl. Surf. Sci. **226**, 242 (2004).